Journal of Human Genetics (2014) 59, 504–511

www.nature.com/jhg

ORIGINAL ARTICLE

Alterations to DNA methylation and expression of *CXCL14* are associated with suboptimal birth outcomes

Clara Y Cheong[1], Keefe Chng[1], Mei Kee Lim[1], Ajith I Amrithraj[2], Roy Joseph[1], Rami Sukarieh[1], Yong Chee Tan[1], Louiza Chan[1], Jun Hao Tan[1], Li Chen[1], Hong Pan[1], Joanna D Holbrook[1], Michael J Meaney[1], Yap Seng Chong[1,2], Peter D Gluckman[1,3] and Walter Stünkel[1]

CXCL14 **is a chemokine that has previously been implicated in insulin resistance in mice. In humans, the role of *CXCL14* in metabolic processes is not well established, and we sought to determine whether *CXCL14* is a risk susceptibility gene important in fetal programming of metabolic disease. For this purpose, we investigated whether *CXCL14* is differentially regulated in human umbilical cords of infants with varying birth weights. We found an elevated expression of *CXCL14* in human low birth weight (LBW) cords, as well as in cords from nutritionally restricted *Macaca fascicularis* macaques. To further analyze the regulatory mechanisms underlying the expression of *CXCL14*, we examined *CXCL14* in umbilical cord-derived mesenchymal stem cells (MSCs) that provide an *in vitro* cell-based system amenable to experimental manipulation. Using both whole frozen cords and MSCs, we determined that site-specific CpG methylation in the C*XCL14* promoter is associated with altered expression, and that changes in methylation are evident in LBW infant-derived umbilical cords that may indicate future metabolic compromise through *CXCL14*.**
Journal of Human Genetics (2014) **59,** 504–511; doi:10.1038/jhg.2014.63; published online 7 August 2014

INTRODUCTION

Suboptimal development during early fetal life because of unfavorable environmental conditions *in utero* poses a risk for the later development of metabolic diseases such as type 2 diabetes mellitus, cardiovascular disease and obesity.[1,2] An adverse fetal environment can result in growth restriction but there is a large body of evidence showing that although fetal growth is a proxy for an adverse fetal environment, long-term consequences can occur in the absence of growth impairment. The factors contributing to the increased disease susceptibility in the affected children likely involve epigenetic mechanisms such as DNA methylation; changes known to be influenced by maternal nutrition.[3] The early identification of children who have been epigenetically programmed by a less than optimal fetal environment could enable early preventive interventions. Indeed, it has previously been shown that epigenetic differences at birth independent of birth weight predict adiposity in later life.[3]

We previously studied the transcriptome and epigenome in umbilical cord tissue obtained from babies enrolled in the Singapore-based longitudinal cohort study GUSTO.[4] Among the differentially expressed transcripts was *CXCL14* that was found to be upregulated in umbilical cords from babies born with low birth weight (LBW) and at early gestational age.[5] *CXCL14* has been shown to mediate insulin sensitivity in fat and muscle tissue, among other pleiotropic functions.[6–9] It is thought that *CXCL14* acts as a regulator of glucose metabolism via an as yet unidentified membrane receptor, establishing a cross-talk between *CXCL14* and insulin pathway signaling that results in the inhibition of glucose uptake. In white adipose tissue, *CXCL14* mediates insulin resistance via chemotactic recruitment of macrophages (reviewed in Hara and Nakayama[7]).

To determine whether *CXCL14* is an early biomarker of metabolic dysfunction in the offspring, we utilized human and non-human primate (NHP) tissues to demonstrate variations in *CXCL14* expression in association with altered maternal nutrition. We report that in addition to changes in *CXCL14* expression, we found associated epigenetic changes within the *CXCL14* gene consistent with altered epigenetic regulation at specific CpGs located proximal to the activator protein 1 (AP1) binding site in the promoter of the gene. Together, these results describe the potential for *CXCL14* as a functionally relevant transcriptional and epigenetic biomarker of metabolic disease that is stably represented across different tissues and ages, and conserved across primate species.

MATERIALS AND METHODS

Clinical populations and sample collection

All umbilical cord specimens were derived from babies born at either the KK Women's and Children's Hospital (KKH) or the National University Hospital

[1]Singapore Institute for Clinical Sciences, Agency for Science Technology and Research (A*STAR), Singapore, Singapore; [2]Department of Obstetrics and Gynaecology, Yong Loo Lin School of Medicine, National University of Singapore, Singapore, Singapore and [3]Liggins Institute, University of Auckland, Auckland, New Zealand
Correspondence: Dr W Stünkel, Growth, Development & Metabolism, Brenner Centre for Molecular Medicine, Singapore Institute for Clinical Sciences, 30 Medical Drive, Singapore 117609, Singapore.
E-mail: Walter_Stunkel@sics.a-star.edu.sg
Received 15 April 2014; revised 1 July 2014; accepted 2 July 2014; published online 7 August 2014

(NUH) in Singapore. These hospitals contribute all the subjects to the GUSTO birth cohort study.[4] Written parental consent to participate in the study was given. Ethical approval was granted by the ethics boards of both KKH and NUH, the centralized Institute Review Board (CIRB) and Domain Specific Review Board (DSRB), respectively.

Umbilical cord-derived mesenchymal stem cells (UC-MSCs)

Umbilical cord specimens were obtained from infants born at the NUH. Ethics approval was granted by the NUH-DSRB and written parental consent and participation was obtained at antenatal checkups, with normal and small-for-gestational age (SGA) infants identified through regular ultrasound scans, and confirmed at birth, where SGA was defined as fetal growth between the 5th and <10th percentile. Primary MSC lines were derived from umbilical cord Wharton's jelly following a normal delivery. The cords were collected and processed to retrieve MSCs according to a previously published protocol.[10] The characterization of these cells has been described in more detail elsewhere.[11] UC-MSC lines were maintained in medium (Dulbecco's modified Eagle's medium high glucose with 20% fetal bovine serum, 2 mmol l^{-1} L-glutamine, 1 × Insulin-Transferrin-Selenium G, 5 ng ml^{-1} basic fibroblast growth factor, 0.1 mmol l^{-1} b-ME, 1 × Antibiotic/antimycotic mix) and cultured for a maximum of 10 passages.

NHP caloric restriction cohorts

All animal procedures were approved by and conducted in compliance with the standards of the Agri-Food and Veterinary Authority of Singapore and the Singapore Health Services Institutional Animal Care and Use Committee (Singhealth IACUC #2008/SHS/418). Sexually mature macaques (*Macaca fascicularis*) were housed in groups of 1 male to 3 females to allow for natural breeding. Early pregnancy detection was achieved by regular ultrasound scans of female breeders. Measurement of the greatest length of the embryo was used to calculate the gestational age. After confirmation of pregnancy, dams were housed in individual cages in a screened roof compound with a daily temperature range of 26–32 °C and constant humidity of 84%. Food intake was individually monitored and regulated throughout pregnancy. Pregnant dams were randomly assigned into caloric restricted or control cohorts. Control dams had access to *ad libitum* food (Laboratory Fiber-Plus, Monkey Diet 5049, LabDiet, St Louis, MO, USA) throughout gestation, whereas nutrient-restricted animals were fed at 65% of control intake from gestational day 32 to 70, and 70% of control intake from gestational day 71 to the end of gestation (term gestation for this species under laboratory conditions is 154–170). Pregnancy was monitored by monthly ultrasound scans, and natural delivery attained for all births without human intervention.

5-Aza-2′-dC treatment of UC-MSCs

MSCs (passage 3) were grown in T75 flasks until confluence and subsequently split into 5 cm dishes. Then, 1 µl of 10 mM 5-aza-2′-deoxycytidine (5-aza-dC) stock in dimethyl sulfoxide was added to 2 ml of MSC medium everyday for 5 days to the treatment group. An equivalent volume of dimethyl sulfoxide was added to the control. At the end of 5 days, cells were harvested in TRIzol (Life Technologies, Carlsbad, CA, USA) for RNA extraction. Cell pellets were washed and frozen for DNA extraction.

RNA extraction

RNA extraction for human and NHP umbilical cords was similarly performed. Briefly, cord tissue was crushed in liquid nitrogen using a mortar and pestle. Crushed cord tissue was transferred to a sterile gentleMACS tube containing TRIzol reagent, and homogenized on the gentleMACS Dissociator (both, Miltenyi Biotech GmBH, Bergisch Gladbach, Germany). After centrifugation to remove cell debris, the supernatant was transferred to a clean tube, and 200 µl chloroform was added per 1 ml of TRIzol used. Samples were vortexed, then centrifuged and the aqueous phase transferred to a new tube. For human samples, an equal volume of isopropanol was added, and RNA left to precipitate overnight at −20 °C. The RNA pellet was retrieved by centrifugation, and washed twice in 70% ethanol, air-dried, and resuspended in 30 µl of RNAse-free water. For NHP samples, an equal volume of 70% ethanol was added to the aqueous phase, mixed gently and applied to an RNeasy mini column (Qiagen, Hilden, Germany). Wash steps were applied according to the manufacturer's recommendation, an on-column DNAse removal step included and RNA was eluted in RNAse-free water. RNA from UC-MSC lines was prepared using a Qiagen RNEasy kit, according to the manufacturer's instructions. In all samples, RNA integrity and concentration was determined using the Agilent 2100 Bioanalyzer RNA 6000 Nano Labchip (Agilent Technologies, Waldbronn, Germany), and RNA purity using a Nanodrop ND-8000 spectrophotometer (Thermo Fisher Scientific, Wilmington, DE, USA).

Quantitative PCR

Complementary DNA was prepared from total RNA, with MuLV-Reverse Transcriptase contained in the High Capacity cDNA Reverse Transcription Kit (Life Technologies). Quantitative PCR reactions were prepared in triplicate using Power SYBR Green Master Mix (Life Technologies) in a final reaction volume of 10 µl. Samples were run on an ABI7900 HT Sequence Detection System (Life Technologies), and primers were previously validated for similar primer efficiencies. Fold change was quantified using the relative Ct method, and group differences verified with Student's *t*-test. Primer sequences are as follows:

Human sequences: CXCL14-F: 5′-GCACCAAGCGCTTCATCAA-3′ and CXCL14-R: 5′-TCGTAGACCCTGCGCTTCTC-3′; GAPDH-F: 5′-GGTGTGA ACCATGAGAAGTATGACA-3′ and GAPDH-R: 5′-GGTGCAGGAGGCATT GCT-3′; ACTB-F: 5′-CGAGGCCCCCCTGAAC-3′ and ACTB-R: 5′-GTCTCAA ACATGATCTGGGTCATC-3′.

M. fascicularis sequences: CXCL14-F: 5′-GTCAGCATGAGGCTCCTG-3′ and CXCL14-R: 5′-GTACTTTGGCTTCATTTCCAG-3′; ACTB-F: 5′-CTGACTACC TCATGAAGATCCTC-3′ and ACTB-R: 5′-TGTTGGCGTACAGGTCTTTAC-3′; GAPD-F: 5′-GTGAAGGTCGGAGTCAACG-3′ and GAPD-R: 5′-ATGGGTGG AATCATACTGGAAC-3′; RPL32-F: 5′-TCAAGGAGTTGGAAGTGCTG-3′ and RPL32-R: 5′-GGGTTGGTGACTCTGATGG-3′.

DNA extraction

DNA extraction for human and NHP umbilical cords was similarly performed. Briefly, cord tissue was crushed in liquid nitrogen using a mortar and pestle. Crushed cord tissue was transferred to a sterile gentleMACS tube containing 10 U ml^{-1} hyaluronidase in 1 × phosphate-buffered saline (Type 1S-hyaluronidase, Cat. no. H4506, Sigma Aldrich, St Louis, MO, USA) and incubated for 30 min at 37 °C with gentle shaking. Thereafter, an equal volume of TNES solution (50 mM Tris pH 7.5, 400 mM NaCl, 100 mM EDTA, 0.5% SDS) was added and homogenized on the gentleMACS dissociator (Miltenyi Biotech GmBH). Proteinase K to a final concentration of 0.1 mg ml^{-1} was added (Roche Holdings AG, Basel, Switzerland), and the sample incubated overnight at 55 °C. High-quality genomic DNA was precipitated with ethanol, and an additional phenol/chloroform step included, before the pelleted DNA was washed with 70% ethanol and resuspended in water. DNA was quantified using Quant-it Picogreen reagent (Life Technologies), purity assessed with a Nanodrop spectrophotometer, and integrity assessed by conventional gel electrophoresis.

Pyrosequencing analysis

Bisulfite conversion of genomic DNA was prepared using a EpiTect Bisulfite Kit (Qiagen) according to the manufacturer's recommendations. Briefly, 500 ng of input genomic DNA was eluted in 20 µl, and 1 µl subsequently used in a PCR reaction for downstream pyrosequencing analysis, and included a biotinylated primer for capture of PCR products to the sepharose beads. PCR products were checked for a specific single band, and pyrosequencing was performed on a PyroMark Q24 machine (Qiagen) using 10–15 µl of PCR product in a standard reaction volume. Primer sequences are available on request.

Molecular cloning and transfection

A fragment of the *CXCL14* promoter was amplified by PCR with primers containing flanking restriction sites for cloning into the pCpG-free vector (Cat. no. PCPGF-PROM, InvivoGen, San Diego, CA, USA) containing a human EF-1alpha promoter and a secreted CpG free allele of the murine embryonic alkaline phosphatase (mSEAP) reporter, genomic position of *CXCL14* fragment:

hg19, chr5(−): 134914698–134914809, 112 bp. This plasmid was subjected to site-directed mutagenesis using the QuikChange Multi Site-Directed Mutagenesis Kit (Agilent Genomics, Santa Clara, CA, USA) at specific CpGs of interest, as indicated in Figure 5a. Thereafter, the verified plasmids were transformed into GT115 *Escherichia Coli*-competent cells (InvivoGen), and purified plasmids obtained using the Qiagen Plasmid Midiprep Kit (Qiagen). Methylation of the plasmids was carried out by treating the plasmids with CpG methyltransferase, *M.SssI* (New England Biolabs, Ipswich, MA, USA) as per the manufacturer's instructions.

HEK-293T cells were seeded at a density of 8×10^4 cells in each well of a 24-well plate in Dulbecco's modified Eagle's medium with 10% heat-inactivated fetal bovine serum. The cells were transfected the next day with 500 ng of pCpG-free plasmids (InvivoGen) per well for 48 h using Lipofectamine LTX (Invitrogen, Carlsbad, CA, USA). Transfection was performed according to the manufacturer's instructions. After 48 h, 20 µl of supernatant from each well was used for detection and quantification of secreted embryonic alkaline phosphatase (mSEAP) activity using QUANTI-Blue (Cat. no. REP-QB1, InvivoGen), performed as per the manufacturer's instructions.

MSCs were similarly transfected using Lipofectamine LTX (Invitrogen), but with an initial seeding density of 50×10^4 cells in a single well of a 12-well plate containing Dulbecco's modified Eagle's medium/10% heat inactivated fetal bovine serum. MSCs were transfected the next day with 1 µg of pCpG-free plasmids. After 96 h, 50 µl of supernatant from each well was used for quantification of secreted mSEAP activity using QUANTI-Blue.

RESULTS

Elevated CXCL14 levels are observed in umbilical cord and cord-derived cells from low birth weight/SGA infants

The transcript abundance of *CXCL14* was first measured in umbilical cords from infants with low and normal birth weights using quantitative PCR. Subjects selected were matched for maternal age, maternal body mass index and gender, and were of single ethnicity (Chinese, Table 1). In this study, we found that the relative levels of *CXCL14* transcript were significantly elevated in infants belonging to the LBW category (birth weight <2500 g), although the fold change differences in the LBW infants varied across a wider spectrum than in normal birth weight infants. We also compared *CXCL14* expression with additional newborn growth parameters, and found that elevated levels of *CXCL14* were indeed associated with overall reduced growth, as measured by smaller head, abdominal and mid-arm circumference, as well as reduced body fat at birth (triceps and subscapular skinfold thickness). Particularly, increased *CXCL14* levels were most significantly correlated with abdominal circumference, a proxy measure for central adiposity (Supplementary Figures 1A–E).

To consider whether the heterogeneity of umbilical cord tissue used might be a contributing factor, we also assessed *CXCL14* expression levels in MSCs derived from the Wharton's jelly of umbilical cords derived from normal and SGA infants (see Materials and methods).

Table 1 Summary of characteristics between normal and low birth weight groups

Group parameter	*Normal birth weight group*	*Low birth weight group*	*P-value*
Maternal age (years)	33.2	33.6	0.428
Maternal BMI	22.0	22.3	0.828
Infant gender (% male)	62.5	50.0	0.464
Gestational age (weeks)	39.0	37.5	0.001

Sample characteristics of the subjects in normal and low birth weight groups show no difference in maternal age, body mass index (BMI), infant gender or ethnicity. There is, however, a significant difference in gestational age, a commonly known covariant with birth weight.

In both the LBW and SGA groups, an increase in *CXCL14* expression was observed, with a median fold increase of approximately threefold in whole umbilical cords (Figure 1a) as well as UC-MSCs (Figure 1b).

Higher *CXCL14* levels in NHPs with SGA background

To ascertain whether the changes in *CXCL14* levels observed in human umbilical cord and UC-MSCs of LBW/SGA infants were robust, we also looked at *CXCL14* levels in umbilical cords obtained from NHPs *M. fascicularis* that are commonly used to understand aspects of primate metabolic disease and reproduction.[12] Normal dams were placed on global caloric restriction from day 35 of gestation to induce intrauterine growth restriction (IUGR) in the offspring, who had marginally reduced birth weights from control offspring (results not published). Umbilical cord levels of *CXCL14* were measured between the induced SGA/IUGR and control offspring, with a clear indication that growth-restricted *Macaca* infants too had significantly elevated *CXCL14* levels (Figure 2) to similar extents observed in human samples (Figure 1). Similar to what we observed in humans, *CXCL14* expression levels in the *Macaca* neonates were also negatively correlated with reduced abdominal circumference at birth (Supplementary Figure 1F).

5-Aza-dC treatment of UC-MSCs induces elevated *CXCL14* expression

In the context of tumorigenesis, depressed *CXCL14* expression has been observed,[13] and was attributed to epigenetic silencing, as the addition of the demethylating agent 5-aza-dC was shown to reactivate *CXCL14* levels with a subsequent increase in *CXCL14* chemoattractant activity.[14] This was accompanied by the identification of promoter-bound CpGs that are hypermethylated in cancer cells.

We sought to see whether *CXCL14* expression was also regulated by DNA methylation in our UC-MSC system. For this purpose, we treated two normal MSC lines with 5-aza-dC. As measured by quantitative PCR, *CXCL14* expression was enhanced following the treatment, suggesting that DNA methylation is indeed implicated in the regulation of *CXCL14* expression in cord-derived MSCs (Figure 3).

Decreased *CXCL14* methylation within the promoter region in LBW individuals

In order to determine the DNA methylation status of the *CXCL14* gene, we assessed selected CpG sites, including regions in the promoter, where methylation changes were previously reported,[14] as well as in the gene body and the 3′-untranslated region. Intriguingly, at 5 of the 30 CpG sites analyzed (Figures 4a and b, CpG sites A–E), DNA methylation levels were significantly decreased in umbilical cords from LBW individuals. These five CpGs correspond primarily to locations within the 5′-untranslated region and the predicted bidirectional promoter located in an intragenic position ∼7 kb downstream of the canonical *CXCL14* 5′-untranslated region (Figure 4, specific positions shown in Figure 4a, CpGs D and E). Two of these five CpGs are proximal to an AP1 binding site within the promoter region (Figure 4a, CpGs B and C). AP1 binding at this site has previously been shown to affect *CXCL14* expression levels,[15] and includes a CpG site within the AP1 binding sequence itself (Figure 4a, CpG F). As such, we sought to see whether changes in DNA methylation at the two noncontiguous CpGs immediately downstream of the AP1 site were also reflected at the CpG site within the AP1 site, and whether DNA methylation variations in the LBW group might be associated with AP1 binding in order to regulate *CXCL14* levels. We found that the CpG within the AP1 site showed no

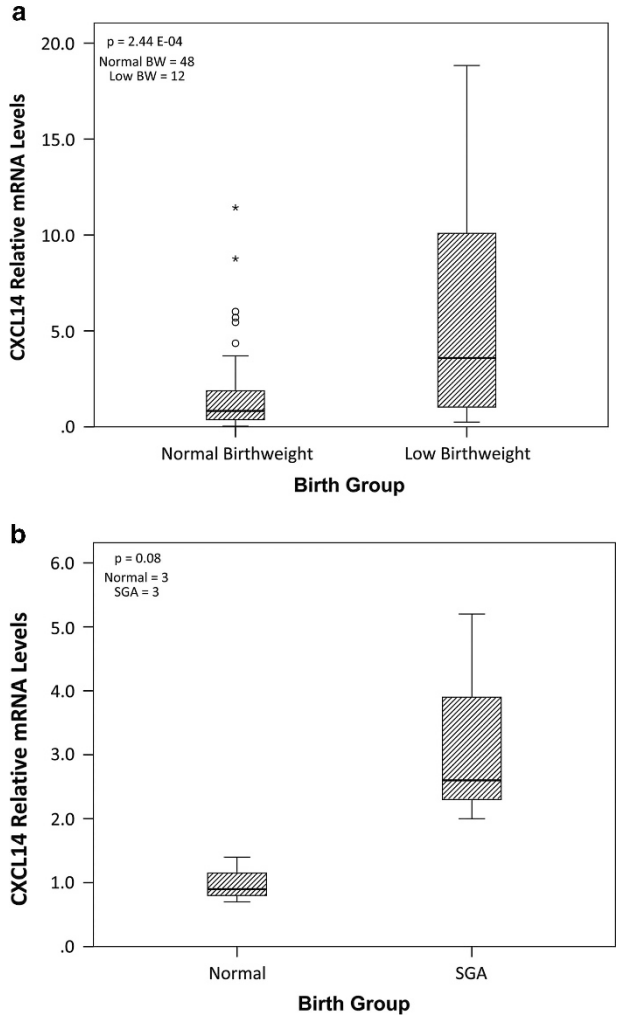

Figure 1 *CXCL14* levels are elevated in low birth weight infants. (**a**) RNA was extracted from whole umbilical cord tissue, and *CXCL14* expression measured by quantitative PCR (qPCR). Each sample was measured in triplicate. Normal birth weight (BW) = 48, low BW = 12, $P = 0.00024$. (**b**) *CXCL14* expression was compared between umbilical cord-derived mesenchymal stem cell (UC-MSC) lines derived from normal and small-for-gestational-age infants (SGA, 5th—10th %tile for birth weight). Normal UC-MSCs = 3, SGA UC-MSCs = 3, Student's *t*-test $P = 0.08$.

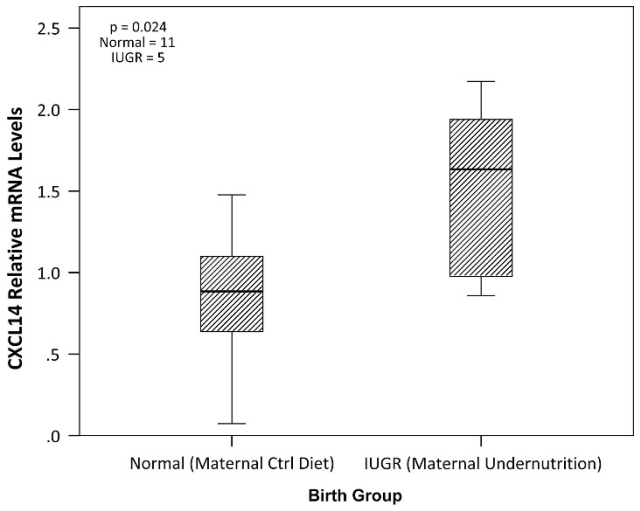

Figure 2 Elevated *CXCL14* expression in non-human primates with intrauterine growth retardation (IUGR). *CXCL14* levels were assessed from whole umbilical cords of Cynomolgus macaques (*Macaca fascicularis*) of normal or small-for-gestational-age (SGA)/IUGR background. In this model, growth restriction in offspring was induced by global maternal undernutrition from gestational day 35 to birth. Normal = 11, IUGR = 5, Student's *t*-test $P = 0.024$.

significant difference in methylation levels between normal and low birth weight subjects (Figure 4b, CpG F).

Mutagenesis of key CpGs within the *CXCL14* promoter alters reporter expression

To verify that specific CpG methylation changes at two sites downstream of the *CXCL14* AP1 binding site contribute directly to changes in *CXCL14* expression, we utilized a reporter assay containing the *CXCL14* region of interest spliced directly upstream of the EF-1alpha promoter and SEAP reporter gene in a CpG-free plasmid. Site-directed mutagenesis of the included *CXCL14* region altered the AP1 proximal CpG or either of the two downstream CpGs to a non-CpG site, rendering each individual site no longer susceptible to methylation after the plasmid was treated with CpG methyltransferase *M.SssI* (Figure 5a).

The *in vitro* methylated and unmethylated reporter plasmids were transfected into HEK293T cells and compared with empty vector controls. On methylation of the wild-type *CXCL14* insert, expression of the reporter decreased by threefold (Figure 5b), in concordance with a typical role for suppressive methylation in the promoter region. Alteration of the AP1 binding site at a non-CpG location resulted in decreased expression to a level similar to that of the methylated wild-type construct, and methylation of the construct further reduced expression. The AP1 binding site of *CXCL14* includes a CpG at the end. To consider whether methylation of this CpG might affect expression, we compared reporter expression of a mutated AP1-CpG to that of a mutated AP1 non-CpG vector. Expression levels were similar when both vectors were compared, either when unmethylated or after methylation *in vitro*. This suggests that loss of AP1 binding, and not methylation changes within the AP1 site, is the primary driver in suppressing *CXCL14* expression. We earlier compared group-wise differences in methylation at the AP1-CpG (Figure 4, CpG F), and also did not find any significant differences in AP1-CpG methylation between normal and low birth weight individuals. We next compared constructs where either of the two CpGs (Figure 4, CpGs B and C) immediately downstream of the AP1 site were altered. Reporter levels were similar between the two CpG sites, suggesting that they may work cooperatively or also function as part of a larger binding site for an unknown factor. When compared with the wild-type construct, the unmethylated constructs showed a significant, although $\sim$12% increase in reporter expression. More notably, expression of the methylated constructs showed that reporter expression was no longer suppressed to a level found for the methylated wild-type construct, and enforced loss of methylation through site-directed mutagenesis at either of these two CpG sites resulted in reporter expression at levels approximately twofold higher than in the wild type. This suggests that methylation at either of the two CpG sites is mechanistically involved in the regulation of *CXCL14* expression at the promoter. In line with this, we discovered that expression of *CXCL14* is elevated in LBW individuals, with associated decrease in methylation at both CpGs B and C.

To ascertain whether this reporter activity might be cell-type specific, we also transfected an umbilical cord-derived MSC line with the same

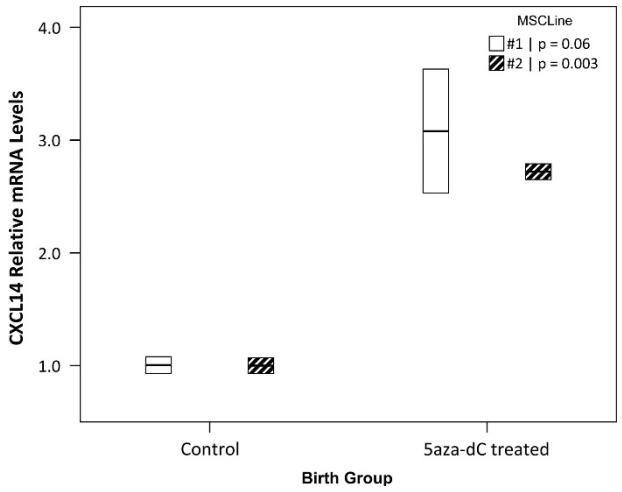

Figure 3 DNA methylation is involved in the regulation of *CXCL14* expression. *CXCL14* expression is increased in mesenchymal stem cells (MSCs) upon treatment with 5-aza-deoxycytidine (5-aza-dC). Results from each independently derived normal umbilical cord-derived MSC (UC-MSC) line show concordance in the direction and extent of change on 5-aza-dC treatment. Technical replicates/cell line = 2, Student's *t*-test $P = 0.06$ (MSC line 1) and $P < 0.05$ (MSC line 2).

constructs, and had largely correspondent findings (Supplementary Figure 2). In UC-MSCs, AP1 binding is still required, and mutation of the binding site at the core or AP1-CpG both result in decreased reporter activity. Although CpGs B and C show similar trends, it is less clear whether there is coordinate activity between the two CpG sites, given that the extent of unmethylated reporter activity differs. In addition, reporter expression of methylated constructs for CpGs B and C show very subtle increases relative to the wild-type equivalent, and may suggest that additional CpG sites, such as those shown in Figure 4b, are implicated in regulating *CXCL14* in this cell type.

DISCUSSION

Using a variety of approaches, our data support an epigenetic mechanism playing a role in the regulation of *CXCL14*, a gene that encodes a chemokine known to function in monocytes and dendritic cell attraction,[16,17] that may also play a role in insulin regulation and obesity.[18] Epidemiological surveys of metabolic dysfunction in adult humans suggest multiple risk factors such as suboptimal fetal nutrition enforcing adaptive response mechanisms leading to SGA neonates.[19–21] Birth weight has often been used as a proxy for the quality of nutritional intake during the fetal period and an adversely low birth weight has typically been associated with a propensity for early catch-up growth and greater abdominal fat mass and elevated risk for subsequent metabolic disease.[22,23] In light of published studies on *Cxcl14*$^{-/-}$ mice that are resistant to the adverse effects of a high-fat diet,[18] we surmised that changes to *CXCL14* levels might be anticipated within a normal human population, as well as in a defined model of nutritionally induced growth restriction in NHPs.

In this study, we examined umbilical cords from human infants, and first found upregulated expression of *CXCL14* in LBW individuals. This agrees with rodent data on *Cxcl14* suggesting a role for this chemokine in weight gain, although particularly in female rodents over males. No such gender association for *CXCL14* expression levels was found in our human umbilical cord data, but this would be better considered over a larger cohort analysis. Separately, it may be that this gender association is not conserved between the species. In our human umbilical cord data (Figure 1a), the difference in *CXCL14* expression levels between low and normal birth weight groups is robust, but shows a larger range of variation in the LBW group. As additional factors besides birth weight would improve the discrimination between metabolic potentials of the individuals surveyed, we also considered other typical neonate anthropometric measures, and found that higher *CXCL14* expression levels were indicative of generally smaller infants with lesser adiposity at birth. This may warrant additional consideration for employing *CXCL14* expression levels as an indicator of an individual's likely metabolic trajectory.

Human umbilical cords are one of the few birth tissues available for routine analysis, and present a snapshot of the gestational health of an infant. However, considering the complexity of multiple cell types in cord might also contribute to the variation seen in *CXCL14* levels, we also analyzed UC-MSCs that originate from the cord's Wharton's jelly component.[24] These multipotent cells potentially contribute to adipocyte and muscle cell lineages, and may provide a more direct comparison of *CXCL14* levels in a single cell line that is relevant to known *CXCL14* function in obesity-related insulin signaling. Reliably, we also obtained a similar mean (approximately threefold) level of *CXCL14* increase in UC-MSCs from SGA infants (Figure 1b). This suggests that UC-MSCs may be successfully used to represent umbilical cords, with the added advantage of *in vitro* manipulation.

Because LBW/SGA designations have been used as proxy parameters, and are possible outcomes, but not causal for true intrauterine growth retardation, we proceeded to analyze umbilical cord specimens obtained from Cynomolgus macaques. The macaques were subjected to controlled nutritional restriction from early gestation onwards so as to develop IUGR in the offspring (Chng K *et al*, manuscript in preparation). We found a significantly increased level of *CXCL14* in the SGA/IUGR offspring, despite the small number of samples inherent in an experimental primate study. Given the subtle phenotypic differences between the SGA/IUGR and normal offspring at birth (data not published), it is of note that early differences in *CXCL14* levels are already recognizable at this stage.

Epigenetic mechanisms have a role in developmental plasticity[25] and might also be at work in the regulation of *CXCL14*. To test this hypothesis, normal UC-MSCs were subjected to treatment with 5-aza-dC, a global nonspecific inhibitor of DNA methylation.[26] Upon treatment, the UC-MSCs showed increased levels of *CXCL14*, suggesting that *CXCL14* is an epigenetically regulated gene and that loss of DNA methylation may contribute to the increased *CXCL14* expression observed in the umbilical cord specimens examined. Although multiple CpGs may be involved in DNA methylation-based control of the locus, we analyzed 30 sites across *CXCL14*, selected to represent CpGs proximal to the promoter, or other landmarks such as insulator binding sites, repetitive sequences and predicted alternative promoter sites. From this, five sites were found to significantly differ between low and normal birth weight groups. Interestingly, these sites all showed the same directionality of methylation change, with a decrease seen in LBW individuals. This may be coincidental, or otherwise represent a larger change in the methylation landscape across *CXCL14* that increases the permittivity of chromatin, although in a more subtle manner than at a single site alone. Given the proximity of these CpG sites in *cis*, further analysis may consider whether these CpG sites work cooperatively, and perhaps show complementary looping that create novel enhancer binding sites.

AP1 binding was previously shown to increase *CXCL14* expression.[15] Of the 5 CpGs analyzed, 2 are located within 20 bp downstream of the published AP1 binding site. We investigated

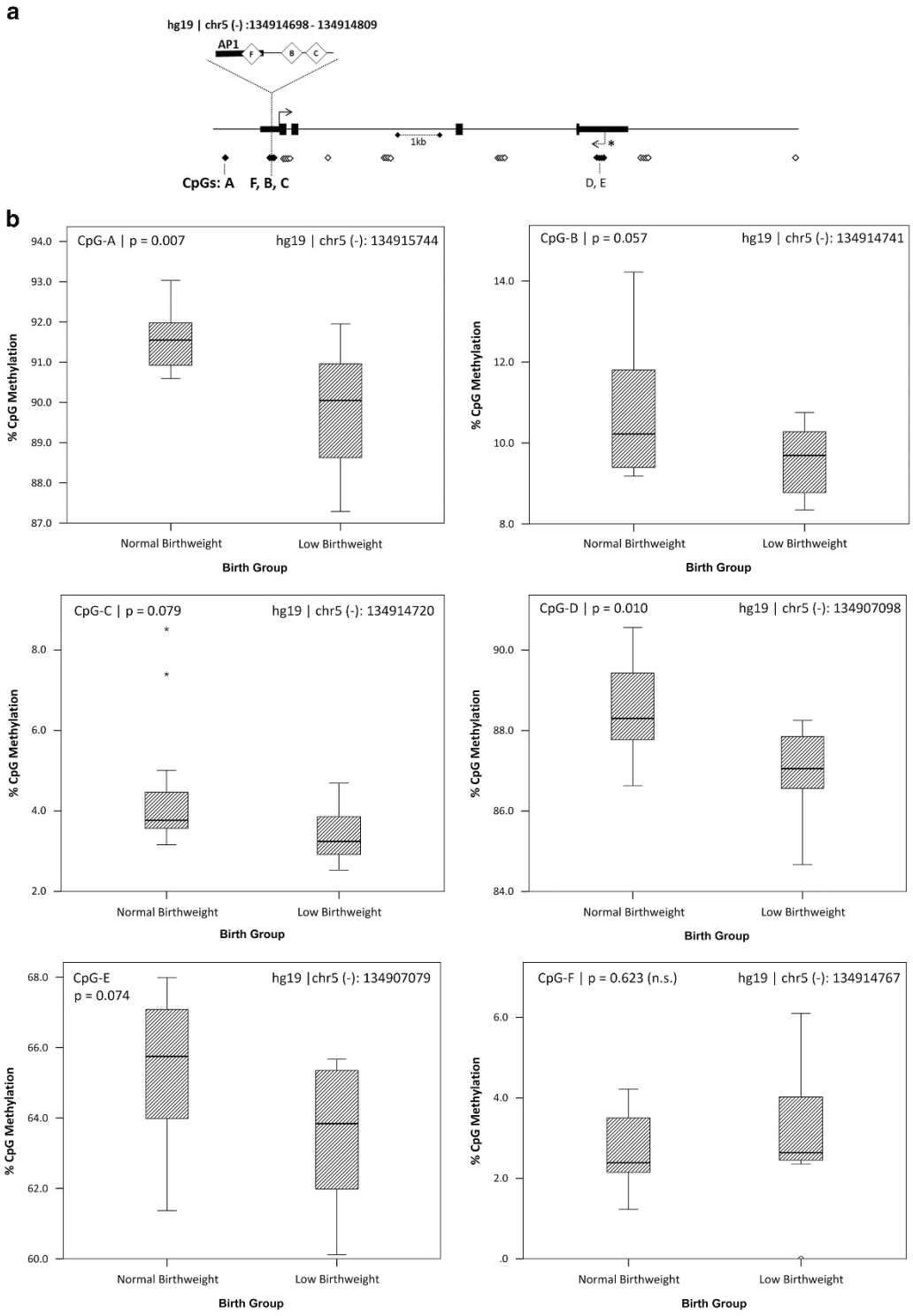

Figure 4 CpG methylation assessed across *CXCL14* identifies variable methylation sites in human umbilical cords. (**a**) Map of *CXCL14* locus with CpGs A–F shown in genomic context (CpGs A–F: filled diamonds). Also, 25 additional CpGs were analyzed in human umbilical cords of normal and low birth weight (BW) backgrounds, all by bisulfite pyrosequencing (relative positions shown as open diamonds). Five CpGs (A–E) differed between birth weight groups. CpG A is located close to a repetitive sequence slightly upstream of the *CXCL14* 5′-untranslated region (5′-UTR). CpGs B and C are located within the 5′ −UTR next to an activator protein 1 (AP1) binding site; CpGs D and E, located at the 5′ end of a predicted bidirectional promoter that has its origins in the 3′ −UTR of the *CXCL14* reference sequence (*). CpG F is located within the reported AP1 site (TGAGTCACCG), the underline indicates the CG site (CpG-F) within the AP1 binding site, and in the vicinity of CpGs B and C. The organization of these CpG sites is more clearly seen in the expanded region shown, the coordinates given are for this expanded region that is also the region used in the reporter constructs shown in Figure 5. (**b**) CpG methylation at each of the five CpGs (A–E) described in (**a**) show a trend of decreased methylation in the low birth weight (LBW) group. Normal BW = 12, low BW = 7, Student's *t*-test *P*-values as shown in individual panels. Genomic coordinates for each of the six CpGs are shown.

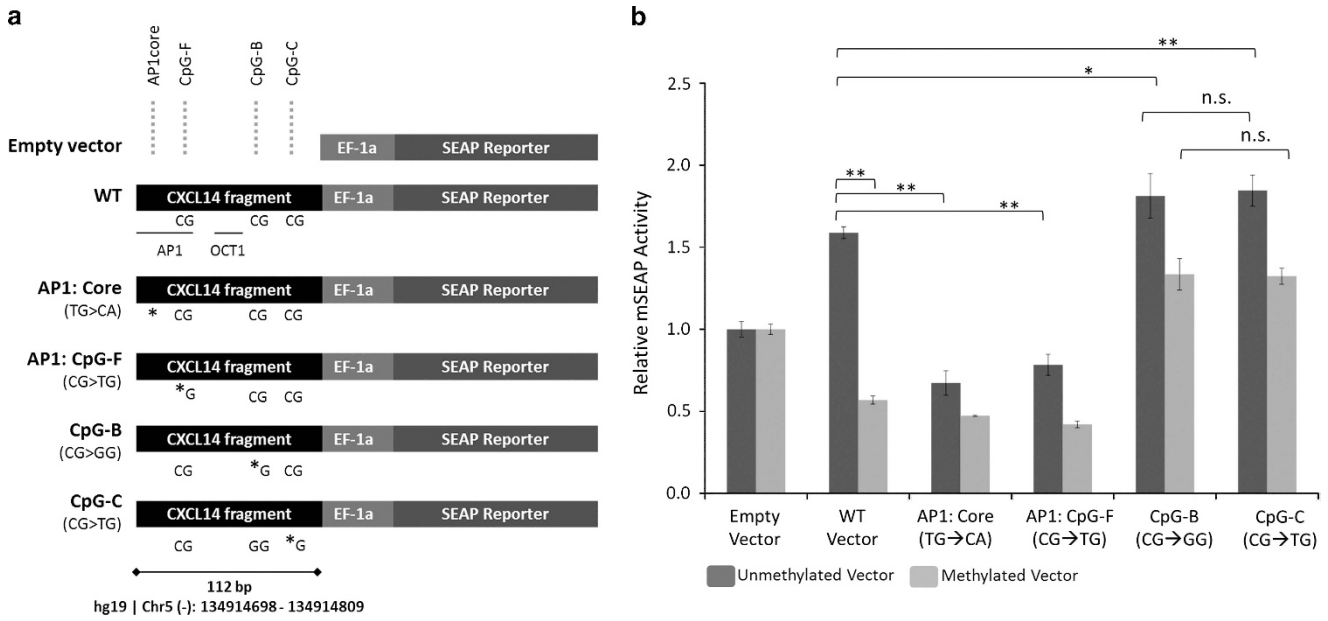

Figure 5 Transient transfection of mutated *CXCL14* promoter identifies two CpGs involved in regulating gene expression. (**a**) Summary of site-directed mutagenesis performed on a set of reporter plasmids containing a *CXCL14* promoter fragment that includes the activator protein 1 (AP1) binding site and CpGs B and C. In each plasmid variant, individual CpG sites were mutated to remove the possibility of methylation when *M.SssI* was used. Reporter activity of the unmethylated and *M.SssI*-treated methylated plasmids was compared to determine the significance of each of the three CpGs in the region toward *CXCL14* activity. (**b**) Transient transfection of *CXCL14* in HEK293T cells. Reporter activity was normalized to empty vector controls for both methylated and unmethylated plasmid variants. Three replicates were performed for each transfection. Student's *t*-test, $*P<0.05$, $**P<0.001$; n.s., not significant.

whether CpG methylation within the AP1 binding site was altered between birth weight groups, but we did not find a significant difference. This was supported by our reporter gene studies, where reporter activity was reduced similarly on mutagenesis of the AP1 binding site, regardless of whether the mutation was placed at the site core or on the CpG at the tail end of the binding site. At the mutated downstream CpG sites, reporter activity was increased over the controls when these sites could no longer be *in vitro* methylated, suggesting that DNA methylation at these specific sites were implicated in the regulation of the downstream promoter. These two CpG sites produced similar results in our reporter assay, and are likely part of the same functional region. In similar transfections of these constructs performed in an UC-MSC line, we note that the results recapitulate the major trends seen in HEK-293T cells, with differences potentially attributable to the presence of additional transcriptional regulatory mechanisms that may be more active in a multipotent cell line.

In conclusion, we have shown that *CXCL14* expression levels are increased in specimens typically associated with a higher risk of developing metabolic disease. This is seen in both human and human-derived samples, and confirmed in a defined SGA/IUGR model using NHPs. The impaired fetal environment results in changes to *CXCL14*, and these may persist through time via epigenetic mechanisms. We have shown that DNA methylation is one such mechanism, although it is likely that additional epigenetic and transcriptional controls are at work, and further studies to probe for changes in histone modifications are pending. Our findings suggest that epigenetic regulation of *CXCL14* expression has a developmental influence on pathways to insulin resistance and suggests approaches to both physiological and interventional studies.

CONFLICT OF INTEREST

The authors declare no conflict of interest.

ACKNOWLEDGEMENTS

We are grateful for the expert technical assistance of Rachel Chew, Tan Li Hua and Yhee Cheng Chng. We thank Professor Kenneth Kwek and the GUSTO study group for enabling the collection of umbilical cord tissue. This work is supported by the Translational Clinical Research (TCR) Flagship Program on Developmental Pathways to Metabolic Disease funded by the National Research Foundation (NRF) and administered by the National Medical Research Council (NMRC), Singapore (NMRC/TCR/004-NUS/2008). SICS Investigators are supported through Agency for Science Technology and Research (A*STAR) funding.

1 Barouki, R., Gluckman, P. D., Grandjean, P., Hanson, M. & Heindel, J. J. Developmental origins of non-communicable disease: implications for research and public health. *Environ. Health.* **11,** 42 (2012).
2 Hanson, M. A. & Gluckman, P. D. Developmental origins of health and disease: moving from biological concepts to interventions and policy. *Int. J. Gynaecol. Obstet.* **115** Suppl 1, S3–S5 (2011).
3 Godfrey, K. M., Sheppard, A., Gluckman, P. D., Lillycrop, K. A., Burdge, G. C., McLean, C. *et al*. Epigenetic gene promoter methylation at birth is associated with child's later adiposity. *Diabetes* **5,** 1528–1534 (2011).
4 Soh, S. E., Tint, M. T., Gluckman, P. D., Godfrey, K. M., Rifkin-Graboi, A., Chan, Y. H. *et al*. Cohort profile: Growing Up in Singapore Towards healthy Outcomes (GUSTO) birth cohort study. *Int. J. Epidemiol.* (e-pub ahead of print 2 August 2013; doi:10.1093/ije/dyt125).
5 Stünkel, W., Pan, H., Chew, S. B., Tng, E., Tan, J. H., Chen, L. *et al*. Transcriptome changes affecting Hedgehog and cytokine signalling in the umbilical cord: implications for disease risk. *PLoS ONE* **7**, e39744 (2012).
6 Hara, T. & Tanegashima, K. Pleiotropic functions of the CXC-type chemokine CXCL14 in mammals. *J. Biochem.* **151,** 469–476 (2012).
7 Hara, T. & Nakayama, Y. CXCL14 and insulin action. *Vitam. Horm.* **80,** 107–23 (2009).

8 Takahashi, M., Takahashi, Y., Takahashi, K., Zolotaryov, F. N., Hong, K. S., Iida, K. *et al.* CXCL14 enhances insulin-dependent glucose uptake in adipocytes and is related to high-fat diet-induced obesity. *Biochem. Biophys. Res. Commun.* **364,** 1037–1042 (2007).
9 Nara, N., Nakayama, Y., Okamoto, S., Tamura, H., Kiyono, M., Muraoka, M. *et al.* Disruption of CXC motif chemokine ligand-14 in mice ameliorates obesity-induced insulin resistance. *J. Biol. Chem.* **282,** 30794–30803 (2007).
10 Fong, C. Y., Subramanian, A., Biswas, A., Gauthaman, K., Srikanth, P., Hande, M. P. *et al.* Derivation efficiency, cell proliferation, freeze-thaw survival, stem-cell properties and differentiation of human Wharton's jelly stem cells. *Reprod. Biomed.* **21,** 391–401 (2010).
11 Sukarieh, R., Joseph, R., Leow, S. C., L, Y., Löffler, M., Aris, I. A. *et al.* Molecular pathways reflecting poor intrauterine growth are found in Wharton's jelly derived mesenchymal stem cells. *Hum. Reprod.* (in press).
12 Bauer, S. A., Arndt, T. P., Leslie, K. E., Pearl, D. L. & Turner, P. V. Obesity in rhesus and cynomolgus macaques: a comparative review of the condition and its implications for research. *Comp. Med.* **61,** 514–526 (2011).
13 Tessema, M., Klinge, D. M., Yingling, C. M., Do, K., Van Neste, L. & Belinsky, S. A. Re-expression of CXCL14, a common target for epigenetic silencing in lung cancer, induces tumor necrosis. *Oncogene* **29,** 5159–5170 (2010).
14 Song, E. Y., Shurin, M. R., Tourkova, I. L., Gutkin, D. W. & Shurin, G. V. Epigenetic mechanisms of promigratory chemokine CXCL14 regulation in human prostate cancer cells. *Cancer Res.* **70,** 4394–4401 (2010).
15 Komori, R. 1, Ozawa, S., Kato, Y., Shinji, H., Kimoto, S. & Hata, R. Functional characterization of proximal promoter of gene for human BRAK/CXCL14, a tumor-suppressing chemokine. *Biomed. Res.* **31,** 123–131 (2010).
16 Kurth, I., Willimann, K., Schaerli, P., Hunzike, T., Clark-Lewis, I. & Moser, B. Monocyte selectivity and tissue localization suggests a role for breast and kidney-expressed chemokine (BRAK) in macrophage development. *J. Exp. Med.* **194,** 855–861 (2001).
17 Schaerli, P., Willimann, K., Ebert, L. M., Walz, A. & Moser, B. Cutaneous CXCL14 targets blood precursors to epidermal niches for Langerhans cell differentiation. *Immunity* **23,** 331–342 (2005).
18 Tanegashima, K., Okamoto, S., Nakayama, Y., Taya, C., Shitara, H., Ishii, R. *et al.* CXCL14 deficiency in mice attenuates obesity and inhibits feeding behavior in a novel environment. *PLoS One* **5** (2010).
19 Gluckman, P. D. & Hanson, M. A. Maternal constraint of fetal growth and its consequences. *Semin. Fetal Neonatal Med.* **9,** 419–425 (2004).
20 Gluckman, P. D. & Hanson, M. A. The consequences of being born small - an adaptive perspective. *Horm. Res.* **65** (Suppl 3), 5–14 (2006).
21 Kerkhof, G. F. & Hokken-Koelega, A. C. Rate of neonatal weight gain and effects on adult metabolic health. *Nat. Rev. Endocrinol.* **8,** 689–692 (2012).
22 Meas, T., Deghmoun, S., Armoogum, P., Alberti, C. & Levy-Marchal, C. Consequences of being born small for gestational age on body composition: an 8-year follow-up study. *J. Clin. Endocrinol. Metab.* **93,** 3804–3809 (2008).
23 Barker, D. J., Gluckman, P. D., Godfrey, K. M., Harding, J. E., Owens, J. A. & Robinson, J. S. Fetal nutrition and cardiovascular disease in adult life. *Lancet* **341,** 938–941 (1993).
24 Batsali, A. K., Kastrinaki, M. C., Papadaki, H. A. & Pontikoglou, C. Mesenchymal stem cells derived from Wharton's Jelly of the umbilical cord: biological properties and emerging clinical applications. *Curr. Stem Cell Res. Ther.* **8,** 144–155 (2013).
25 Gluckman, P. D., Hanson, M. A. & Low, F. M. The role of developmental plasticity and epigenetics in human health. *Birth Defects Res. C Embryo Today* **93,** 12–18 (2011).
26 Singh, V., Sharma, P. & Capalash, N. DNA methyltransferase-1 inhibitors as epigenetic therapy for cancer. *Curr. Cancer Drug Targets.* **13,** 379–399 (2013).

Supplementary Information accompanies the paper on Journal of Human Genetics website (http://www.nature.com/jhg)